PHYSICAL REVIEW D **85,** 095021 (2012)

$H \to \gamma\gamma$ in the inert Higgs doublet model

Abdesslam Arhrib,[1,2,*] Rachid Benbrik,[2,3,4,†] and Naveen Gaur[5,‡]

[1]*Faculté des Sciences et Techniques, B. P. 416, Tangier, Morocco*
[2]*LPHEA, FSSM, Cadi Ayyad University, B. P. 2390, Marrakesh, Morocco*
[3]*Instituto de Física de Cantabria (CSIC-UC), Santander, Spain*
[4]*Faculté Polydisciplinaire de Safi, Sidi Bouzid B. P. 4162, 46000 Safi, Morocco*
[5]*Department of Physics, Dyal Singh College (University of Delhi), Lodi Road, New Delhi—110003, India*

(Received 17 January 2012; published 24 May 2012)

Motivated by the recent results from LHC on the di-photon search for a standard model (SM) Higgs-like boson, in this work we discuss the implications of this signal in the framework of the inert Higgs doublet model. Our analysis takes account of the previous limits from Higgs searches at LEP, the Tevatron, and the LHC. We have also considered the bounds coming from perturbativity, unitarity, vacuum stability, and electroweak precision tests. We show that the charged Higgs contributions can interfere constructively or destructively with the W gauge bosons' loops leading to enhancement or suppression of the di-photon rate with respect to the SM rate. We show also that the invisible decay of the Higgs, if open, could affect the total width of the SM Higgs boson and therefore suppress the di-photon rate.

DOI: 10.1103/PhysRevD.85.095021 PACS numbers: 12.60.Fr, 14.80.Ec

I. INTRODUCTION

The LHC in pp collision at 7 TeV has already delivered an integrated luminosity of more than 5 fb^{-1}. Based on this data the ATLAS [1] and CMS [2] collaborations recently have presented their combined and updated results of standard model (SM) Higgs boson searches. Both of the collaborations attempted to search for the SM Higgs boson in mass range 110-600 GeV, the main channels used by them for the analysis are:

(i) *ATLAS* [1] $H \to ZZ^* \to 4\ell$ and $H \to \gamma\gamma$ with full data set of 4.8 fb^{-1} and 4.9 fb^{-1} respectively. Update of $H \to WW^* \to \ell\nu\ell\nu$, $H \to ZZ^* \to 2\ell 2\nu$, $H \to ZZ^* \to 2\ell 2q$ with 2.1 fb^{-1}. They reported an excess of events around the Higgs mass of 126-127 GeV with the maximum local significance level of 2.6 σ.

(ii) *CMS* [2]: $H \to \gamma\gamma$, $H \to bb$, $H \to ZZ^* \to 4\ell$, $H \to 2\ell 2\tau$ at 4.7 fb^{-1} and $H \to \tau\tau$, $H \to WW^* \to 2\ell 2\nu$, $H \to ZZ^* \to 2\ell 2\nu$, $H \to ZZ^* \to 2\ell 2q$ at 4.6 fb^{-1}. They reported a local significance of 2.4 σ around the Higgs mass of 124 GeV.

Note that both CMS and ATLAS have reported some excess at the low mass Higgs boson with low statistical significance in the WW^* and ZZ^* channels. Moreover, from the di-photon channel, ATLAS and CMS have excluded an SM Higgs in the narrow mass range of 114–115 GeV for ATLAS and 127–131 GeV for CMS, at the 95% C.L. With 4.9 fb^{-1} data sets using the combined channels, both ATLAS and CMS have further narrowed down the mass window for the SM Higgs by excluding the mass ranges 131–237 GeV, 251–453 GeV [1], and 127–600 GeV [2] at the 95% C.L.

The effective cross section of di-photon ($\gamma\gamma$) mode can be estimated by inclusive process $\sigma^{\gamma\gamma} = \sigma(pp \to H) \times Br(H \to \gamma\gamma)$. This ($\sigma^{\gamma\gamma}$) could provide possibly the best mode to search for light Higgs boson in mass range 110-140 GeV. ATLAS [3] reported 95% C.L. exclusion limit of $\sigma^{\gamma\gamma}/\sigma^{\gamma\gamma}_{\rm SM} \sim 1.6 - 1.8$ in mass range 110-130 GeV. On the other hand, CMS [4] reported the exclusion limit of $\sigma^{\gamma\gamma}/\sigma^{\gamma\gamma}_{\rm SM} \sim 1.5 - 2$ in mass range 110-140 GeV.

Dark matter (DM) and electroweak symmetry breaking (EWSB) are two of the most important areas of research in particle physics and cosmology. One of the main goals of the LHC is to discover the Higgs boson and hence provide information about the EWSB mechanism. A DM particle is expected to be a weakly interacting massive particle (WIMP) with mass around EWSB scale. In the SM the EWSB is achieved by a Higgs doublet developing a vacuum expectation value (vev). The inert Higgs doublet model (IHDM) is a very simple extension of the SM proposed by Deshpande and Ma [5] that can possibly give a DM candidate. The IHDM is basically a two Higgs doublet model with an imposed Z_2 symmetry. Because of the imposed Z_2 symmetry the IHDM exhibits very interesting phenomenology by predicting a heavy scalar field as a WIMP candidate. The rich phenomenology of the IHDM had been extensively discussed in the context of DM phenomenology [6,7], neutrino mass [8], naturalness [9], and colliders [10,11].

In this work we will analyze the effect of the IHDM on $H \to \gamma\gamma$ in the light of recent results on the Higgs boson searches from the LHC. This effect will mainly come from charged Higgs boson contributions as well as from the total decay width of the Higgs boson in case the invisible decay of the Higgs into dark matter is open. In this study we will

*aarhrib@ictp.it
†rbenbrik@ictp.it
‡gaur.nav@gmail.com

show that the IHDM cannot only account for the excess in the di-photon cross section reported by ATLAS/CMS but can also account for a deficit in the di-photon cross section without modifying the gluon fusion rate and the other decay channels like $h \to b\bar{b}$, $\tau^+\tau^-$, WW^*, ZZ^*.

The paper is organized as follows: In Sec. II we will give the details of the IHDM. Section III is devoted to theoretical and experimental constraints, while in Sec. IV we give details of the evaluation of $h \to \gamma\gamma$ as well as the phenomenological observable at the LHC. In Sec. V we will present our numerical analysis, and finally we conclude in Sec. VI.

II. INERT HIGGS DOUBLET MODEL

The inert Higgs doublet model (IHDM) [5] is an extension of the SM Higgs sector that provides a neutral scalar DM candidate. Apart from the SM Higgs doublet H_1 the model has an additional Higgs doublet H_2. In addition there is a Z_2 symmetry under which all the SM fields and H_1 are even while $H_2 \to -H_2$. We further assume that Z_2 symmetry is not spontaneously broken, i.e.. the H_2 field does not develop a vacuum expectation value (vev). These doublets in terms of physical fields can be parametrized as

$$H_1 = \begin{pmatrix} \phi_1^+ \\ v/\sqrt{2} + (h + i\chi)/\sqrt{2} \end{pmatrix}, \qquad H_2 = \begin{pmatrix} \phi_2^+ \\ (S + iA)/\sqrt{2} \end{pmatrix}. \tag{1}$$

The Z_2 symmetry naturally imposes the flavor conservation. The scalar potential allowed by Z_2 symmetry can be written as

$$\begin{aligned} V = {} & \mu_1^2|H_1|^2 + \mu_2^2|H_2|^2 + \lambda_1|H_1|^4 + \lambda_2|H_2|^4 \\ & + \lambda_3|H_1|^2|H_2|^2 + \lambda_4|H_1^\dagger H_2|^2 \\ & + \frac{\lambda_5}{2}\{(H_1^\dagger H_2)^2 + \text{H.c.}\}. \end{aligned} \tag{2}$$

The electroweak gauge symmetry is broken by

$$\langle H_1 \rangle = \begin{pmatrix} 0 \\ v/\sqrt{2} \end{pmatrix} \quad , \qquad \langle H_2 \rangle = \begin{pmatrix} 0 \\ 0 \end{pmatrix}. \tag{3}$$

This pattern of symmetry breaking ensures unbroken Z_2 symmetry and results in two CP even neutral scalars (h, S) one CP odd neutral scalar (A) in addition to a pair of charged scalars ($H^\pm$). There is no mixing between the two doublets and hence h plays the role of the SM Higgs boson. The remaining Higgs bosons, namely S, A, and $H^\pm$, are ''inert,'' and they do not have any interaction with quarks and leptons. The Z_2 symmetry also ensures the stability of the lightest scalar (S or A) that can act as a dark matter candidate. This aspect has been extensively analyzed in many works while exploring DM phenomenology of the IHDM [6]. The masses of all these six scalars can be written in terms of six parameters[1] namely.

$$\{\mu_2^2, \lambda_1, \lambda_2, \lambda_3, \lambda_4, \lambda_5\}. \tag{4}$$

It is possible to write the quartic coupling λ_i in terms of physical scalar masses and μ_2 as follows:

$$\lambda_1 = \frac{m_h^2}{2v^2} \quad , \qquad \lambda_3 = \frac{2}{v^2}(m_{H^\pm}^2 - \mu_2^2), \tag{5}$$

$$\lambda_4 = \frac{(m_S^2 + m_A^2 - 2m_{H^\pm}^2)}{v^2} \quad , \qquad \lambda_5 = \frac{(m_S^2 - m_A^2)}{v^2}. \tag{6}$$

For our analysis we will take the six independent parameters to be the physical scalar Higgs boson masses, λ_2 and μ_2, i.e. :

$$\{\mu_2^2, m_h, m_S, m_A, m_{H^\pm}, \lambda_2\}. \tag{7}$$

III. THEORETICAL AND EXPERIMENTAL CONSTRAINTS

The parameter space of the scalar potential of the IHDM is constrained both by theoretical considerations as well as by direct experimental searches. From the theoretical constraints which the IHDM is subjected to the most important are the ones that ensure tree-level unitarity and vacuum stability of the theory:

(i) *Perturbativity*: We force the scalar potential to be perturbative by requiring that all quartic couplings of the scalar potential Eq. (2), obey.

$$|\lambda_i| \leq 8\pi. \tag{8}$$

(ii) *Vacuum stability*: To get a potential V bounded from below we obtain the following constraints on the IDHM parameters:

$$\lambda_{1,2} > 0 \quad \text{and} \quad \lambda_3 + \lambda_4 - |\lambda_5| + 2\sqrt{\lambda_1\lambda_2} > 0 \quad \text{and} \quad \lambda_3 + 2\sqrt{\lambda_1\lambda_2} > 0. \tag{9}$$

(iii) *Unitarity*: To constrain the scalar potential parameters of the IHDM one can demand that tree-level unitarity is preserved in a variety of scattering processes namely: scalar-scalar scattering, gauge boson-gauge boson scattering, and scalar-gauge boson scattering. We will follow the technique developed in [12] and therefore we limit ourselves to pure scalar scattering processes dominated by quartic interactions.
The full set of scalar scattering processes can be expressed as an S matrix 22×22 composed of four submatrices which do not couple with each other due to charge conservation and CP-invariance [13,14]. The entries are the quartic couplings which mediate the scattering processes.
The eigenvalues are:

$$e_{1,2} = \lambda_3 \pm \lambda_4 \quad , \qquad e_{3,4} = \lambda_3 \pm \lambda_5 \tag{10}$$

[1] μ_1^2 is constrained by EWSB condition $v^2 = -\mu_1^2/\lambda_1$

$$e_{5,6} = \lambda_3 + 2\lambda_4 \pm 3\lambda_5\,,$$
$$e_{7,8} = -\lambda_1 - \lambda_2 \pm \sqrt{(\lambda_1 - \lambda_2)^2 + \lambda_4^2} \quad (11)$$

$$e_{9,10} = -3\lambda_1 - 3\lambda_2 \pm \sqrt{9(\lambda_1 - \lambda_2)^2 + (2\lambda_3 + \lambda_4)^2} \quad (12)$$

$$e_{11,12} = -\lambda_1 - \lambda_2 \pm \sqrt{(\lambda_1 - \lambda_2)^2 + \lambda_5^2}. \quad (13)$$

We impose perturbative unitarity constraint on all e_i's.

$$|e_i| \leq 8\pi, \forall i = 1, \ldots, 12; \quad (14)$$

the strongest constraint on $\lambda_{1,2}$, 2 comes from $e_{9,10}$ which gives

$$\lambda_1 + \lambda_2 \leq \frac{8\pi}{3}. \quad (15)$$

(iv) *Electroweak precision tests*: A common approach to constrain physics beyond the SM is by using the global electroweak fit through the oblique S, T, and U parameters [15]. In the SM the EWPT implies a relation between m_h and m_Z. In this model, there is also a relation among the masses. It follows from the expression for S and T given by

$$T = \frac{1}{32\pi^2\alpha v^2}[F(m_{H^\pm}^2, m_A^2) + F(m_{H^\pm}^2, m_S^2) - F(m_A^2, m_S^2)] \quad (16)$$

and,

$$S = \frac{1}{2\pi}\left[\frac{1}{6}\log\left(\frac{m_S^2}{m_{H^\pm}^2}\right) - \frac{5}{36} + \frac{m_S^2 m_A^2}{3(m_A^2 - m_S^2)^2} + \frac{m_A^4(m_A^2 - 3m_S^2)}{6(m_A^2 - m_S^2)^3}\log\left(\frac{m_A^2}{m_S^2}\right)\right] \quad (17)$$

where the function F is defined by

$$F(x, y) = \begin{cases} \frac{x+y}{2} - \frac{xy}{x-y}\log(\frac{x}{y}), & x \neq y \\ 0, & x = y \end{cases}. \quad (18)$$

For the purpose of this paper, we will use the PDG values of S and T with U fixed to be zero [16,17]. We allow S and T parameters to be within 95% C.L. The central value of S and T, assuming a SM Higgs mass of $m_{H_{\rm SM}} = 117$ GeV, is given by [16]:

$$S = 0.03 \pm 0.09, \qquad T = 0.07 \pm 0.08 \quad (19)$$

with a fit correlation of 87%. One can obtain a bound on $m_{H^\pm}$ by using unitarity and vacuum stability constraints. Note that we can restore custodial symmetry in the scalar potential of the IHDM by taking $m_{H^\pm}^2 = m_A^2$.

(v) *Experimental constraints*: Here we will discuss the experimental constraints from direct searches on the masses of the IHDM. In the case of the SM Higgs (h), we can use CMS and ATLAS constraints discussed in Sec. I when the non-SM Higgs decays such as $h \to SS$, $h \to H^+H^-$, $h \to A^0A^0$ are kinematically forbidden. In the case where one or more of these decay modes are kinematically allowed with a substantially large branching ratio, it will suppress the other SM decays and hence one can evade the present constraints on the SM Higgs which are based on conventional SM Higgs decays like $h \to b\bar{b}$, $h \to \tau^+\tau^-$, $h \to WW^*$, and $h \to ZZ^*$ (see Fig. 3). From the precise measurement of W and Z widths, one can get additional constraints on the Higgs masses by demanding that the decays $W^\pm \to \{SH^\pm, A^0H^\pm\}$ and/or $Z \to \{SA^0, H^+H^-\}$ are forbidden. This leads to the following constraints on the mass spectrum of Higgs bosons: $m_S + m_{H^\pm} > m_W$, $m_A + m_{H^\pm} > m_W$, $m_A + m_S > m_Z$, and $m_{H^\pm} > m_Z/2$ [16]. Note that LEP, Tevatron, and LHC bounds on $H^\pm$ and A^0 will not apply here because the standard search channels assumes those scalars decaying into a pair of fermions which are absent in the IHDM due to Z_2 symmetry. In the IHDM, the charged Higgs $H^\pm$ can decay into $H^\pm \to W^\pm A^0$ followed by $A^0 \to SZ$ or $H^\pm \to W^\pm S$. Therefore the decay product of the production processes $e^+e^-/pp \to H^+H^-$, $e^+e^-/pp \to SA^0$ would be missing energy and multileptons or multijets depending on the decay product of W and Z. Such a signature would be similar to some extent to the supersymmetric searches for charginos and neutralinos at e^+e^- or at hadron colliders [11]. Taking into account those considerations, we will assume that $m_{H^\pm} > 70$ GeV (see [11] for more details).

IV. $h \to \gamma\gamma$ IN THE IHDM

It is well known that LHC searches for the low-mass SM Higgs ($m_H \in [110, 140]$ GeV) are the most challenging especially at low luminosities. In this low-mass region, the main search is through the di-photons which can be complemented by the $\tau^+\tau^-$ mode and potentially with the $b\bar{b}$ mode, while the WW^*, ZZ^* channels are already competitive in the upper edge (130–140 GeV) of this mass range [18].

The results of the SM predictions for the one-loop induced $h \to \gamma\gamma$ are well known [19]. In the SM the rate for $h \to \gamma\gamma$ is dominated by the W loops and the branching ratio of this channel is of the order of $\sim 2 \times 10^{-3}$. Several studies have been carried out looking for large loop effects beyond the SM. Such large effects can be found in various extensions of the SM, such as the minimal supersymmetric standard model (MSSM) [20], the next-to-MSSM [21], the two Higgs doublet model [22–24], the little Higgs models

[25], extra-dimensions [26], and in models with triplet Higgs [27].

In the IHDM, the partial width of $h \to \gamma\gamma$ receives an additional contribution from the charged Higgs boson loop which can both enhance or suppress the width compared to the SM. It can be expressed as [28]:

$$\Gamma(h \to \gamma\gamma) = \frac{\alpha^2 G_F m_h^2}{128\sqrt{2}\pi^3} \left| \sum_i N_{ci} Q_i^2 F_i + g_{hH^\pm H^\mp} \frac{m_W^2}{m_{H^\pm}^2} F_0(\tau_{H^\pm}) \right|^2, \quad (20)$$

where N_{ci}, Q_i are the color factor and the electric charge, respectively, for a particle i running in the loop. The dimensionless loop factors for particles of given spin in the subscript are

$$\begin{aligned} F_1 &= 2 + 3\tau + 3\tau(2-\tau) f(\tau), \\ F_{1/2} &= -2\tau[1 + (1-\tau) f(\tau)], \\ F_0 &= \tau[1 - \tau f(\tau)], \end{aligned} \quad (21)$$

with

$$f(\tau) = \begin{cases} [\sin^{-1}(1/\sqrt{\tau})]^2, & \tau \geq 1 \\ -\frac{1}{4}[\ln(\eta_+/\eta_-) - i\pi]^2, & \tau < 1 \end{cases} \quad (22)$$

and

$$\tau_i = 4m_i^2/m_h^2, \qquad \eta_\pm = 1 \pm \sqrt{1-\tau}. \quad (23)$$

In Eq. (20), the coupling $g_{hH^\pm H^\mp}$ is given by

$$g_{hH^\pm H^\mp} = -2i\frac{m_W s_W}{e}\lambda_3 = -i\frac{e}{2 s_W m_W}(m_{H^\pm}^2 - \mu_2^2). \quad (24)$$

It is clear from the above Eq. (24) that the coupling of the SM Higgs boson to a pair of charged Higgs is completely fixed by the λ_3 parameter. As we shall see later, the sign of λ_3 will play an important role in the calculation of the partial width of $h \to \gamma\gamma$.

At the collider one measures the total cross section $\sigma_h^{\gamma\gamma} = \sigma(pp \to h \to \gamma\gamma)$. The largest contribution to the production cross section for this observable $\sigma_h^{\gamma\gamma}$ is through gluon fusion, $gg \to h \to \gamma\gamma$. For phenomenological purposes, we define the ratio of the di-photon cross section normalized to the SM rate as follows:

$$R_{\gamma\gamma} = \frac{\sigma_h^{\gamma\gamma}}{\sigma_{h_{\rm SM}}^{\gamma\gamma}} = \frac{\sigma(gg \to h) \times Br(h \to \gamma\gamma)}{\sigma(gg \to h)^{SM} \times Br(h \to \gamma\gamma)^{SM}} = \frac{Br(h \to \gamma\gamma)}{Br(h \to \gamma\gamma)^{SM}}, \quad (25)$$

where we have used the narrow width approximation in the first line of Eq. (25) while we have used the fact that $\sigma(gg \to h)$ is the same both in the IHDM and SM. Hence one can conclude that the ratio $R_{\gamma\gamma}$ in the IHDM depends only on the branching ratio of $h \to \gamma\gamma$. In the evaluation of the branching ratios, we use for the total decay widths the following expressions:

$$\Gamma_h^{SM} = \sum_{f=\tau,b,c} \Gamma(h \to ff) + \Gamma(h \to WW^*) + \Gamma(h \to ZZ^*) + \Gamma(h \to gg) + \Gamma(h \to \gamma\gamma) \quad (26)$$

$$\Gamma_h^{IHDM} = \Gamma_h^{SM} + \sum_{\Phi=S,A,H^\pm} \Gamma(h \to \Phi\Phi) \quad (27)$$

where the expressions for the scalar decay widths are taken from [28]. Note that all the decay modes $h \to SS$, $h \to A^0A^0$, and $h \to H^\pm H^\mp$ might not be kinematically allowed. In the case where the DM particle is lighter than $m_h/2$, the decay $h \to SS$ is kinematically allowed and could give substantial contribution to the total width of the Higgs. The analytical expression for hSS coupling in the IHDM can be written as

$$g_{hSS} = -2i\frac{m_W s_W}{e}\lambda_L = -i\frac{e}{s_W m_W}(m_S^2 - \mu_2^2) \quad (28)$$

which is proportional to $(m_S^2 - \mu_2^2)$, with $\lambda_L = \lambda_3 + \lambda_4 + \lambda_5$.

V. NUMERICAL RESULTS

Before presenting our numerical results we would like to point out that in Ref. [22] $h \to \gamma\gamma$ has been studied in 2HDM type I as well as in the IHDM. But, Ref. [22] only focused on the IHDM parameter space region where only the SM Higgs boson decays, namely $h \to \tau^+\tau^-$, $b\bar{b}$, $c\bar{c}$, W^+W^-, ZZ, $\gamma\gamma$, and gg decays of the SM Higgs are kinematically allowed. In this case, the total width of the Higgs boson is the same in the SM and in the IHDM, and therefore our ratio $R_{\gamma\gamma}$ given in Eq. (25) reduces to $\Gamma(h \to \gamma\gamma)/\Gamma(h \to \gamma\gamma)^{SM}$ as defined in Ref. [22]. Our results agree with the results given in [22]. In the case where $h \to SS$ is open, the ratio $\Gamma(h \to \gamma\gamma)/\Gamma(h \to \gamma\gamma)^{SM}$ is not the appropriate one to be compared with CMS and ATLAS data but rather the ratio of the branching ratio as defined in Eq. (25). In this section we will discuss the effect of the IHDM input parameters as defined in Eq. (7) on $R_{\gamma\gamma}$. We will also comment on constraints coming from WIMP relic density. As shown in Fig. 3 we can have a very interesting situation of evading the LHC bounds on SM Higgs in the region of IHDM parameter space where the invisible decay of Higgs ($h \to SS$) is kinematically allowed. This issue will be discussed in detail in forthcoming work [29].

In our numerical analysis, we perform a systematic scan over the parameter space of the IHDM. We vary the model parameters in the range

$$\begin{aligned} 110\ \text{GeV} \leq m_h \leq 150\ \text{GeV} \qquad & 5\ \text{GeV} \leq m_S \leq 150\ \text{GeV} \\ 70\ \text{GeV} \leq m_{H^\pm}, \qquad & m_A \leq 1000\ \text{GeV}, \\ -500\ \text{GeV} \leq \mu_2 \leq 500\ \text{GeV}, \qquad & 0 \leq \lambda_2 \leq 8\pi. \end{aligned} \quad (29)$$

In addition we have imposed $m_S < m_A$ and $m_S < m_{H^\pm}$ and $m_S < m_h$. This mass hierarchy ensures that m_S will be the

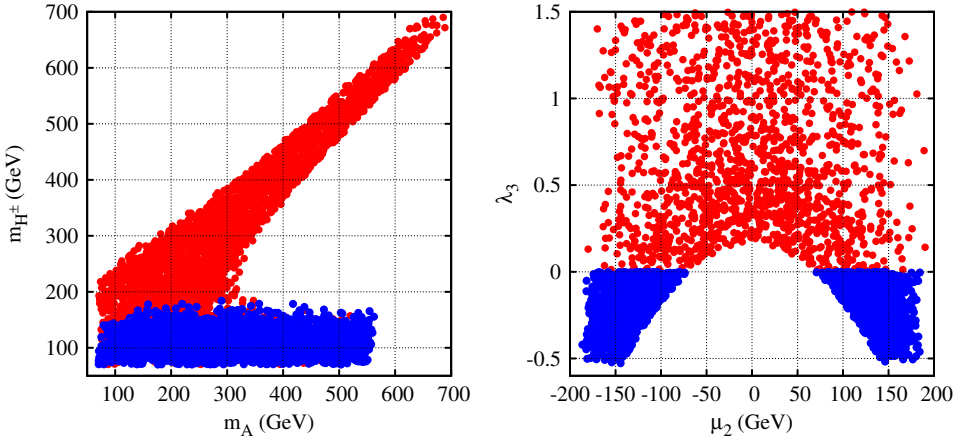

FIG. 1 (color online). The allowed parameter space in the $(m_A, m_{H^\pm})$ plane (left panel) and (μ_2, λ_2) plane (right panel) taking into account theoretical and experimental constraints. The red dots represent $R_{\gamma\gamma} < 1$ and blue dots represent $R_{\gamma\gamma} > 1$.

WIMP DM candidate. These values cover essentially the entire physically interesting range of parameters in the IHDM. For SM Higgs (h) we have specifically chosen a range where $h \to \gamma\gamma$ could be an important channel (light Higgs boson mass) and the region that shows some deviations from SM as reported in recent LHC results [3,4]. We have imposed the theoretical constraints mentioned in previous sections as well as constraints form oblique parameters S and T. In addition, we would like to stress that the coupling hSS, which is proportional to $\lambda_L = \lambda_3 + \lambda_4 + \lambda_5$ (see Eq. (28)), substantially affects the WIMP relic density [7]. It has been show in [7] that with light Higgs boson $m_h \sim 120$ GeV and $m_S \sim 60$–80 GeV the relic density would be consistent with experimental data for $|\lambda_L| < 0.2$.In the following numerical analysis, with low Higgs mass 115–140 GeV, we will impose rather conservative limit on $|\lambda_L| < 0.5$. With all the above constraints imposed, we get the following limits: $\lambda_2 < 4\pi/3$, $m_{H^\pm}, m_A < 700$ GeV, and $|\mu_2| < 200$ GeV. In all scatter plots, the red and blue dots shown in Figs. 1 and 2, 4,5 represent $R_{\gamma\gamma} < 1$ and $R_{\gamma\gamma} > 1$ respectively.

In Figure. 1, we show the allowed region in the $(m_A, m_{H^\pm})$ (left panel) and $(m_S, m_{H^\pm})$ (right panel). The perturbativity and vacuum stability constraints together dramatically reduce the allowed parameter space of the model. In particular, the perturbativity and vacuum stability constraints exclude the large values of charged Higgs mass $m_{H^\pm}$ and CP-odd mass m_A while the EWPT measurement constraint mainly splits between the scalar masses. Accordingly, an enhancement in $R_{\gamma\gamma}$ is possible for a relatively light charged Higgs mass. In the right panel of Fig. 1 we show the scatter plot in (μ_2, λ_3) space. As can be seen again from this figure the enhancement in $R_{\gamma\gamma}$ is possible only for negative values of λ_3. Note that the plots are symmetric under $\mu_2 \to -\mu_2$.

In Fig. 2, we illustrate $R_{\gamma\gamma}$ as a function of $|\lambda_L| < 0.5$ which is one of the main parameters contributing to the WIMP relic density calculation. For large and negative λ_L one can see that $R_{\gamma\gamma}$ can reach 1.6 while for large and positive λ_L, $R_{\gamma\gamma}$ can be of the order 0.7. It is clear from this plot that even for small $|\lambda_L| < 0.2$, which might be needed to accommodate WIMP relic density [7], we can still have both $R_{\gamma\gamma} < 1$ and >1.

As discussed in Sec. I due the presence of Z_2 symmetry in the IHDM the lightest Higgs boson could be a stable particle. With the spectrum we have chosen the lightest Z_2 odd Higgs boson is the neutral scalar S and hence the SM Higgs will have an invisible decay mode, namely $h \to SS$. For illustration, in Fig. 3, we have fixed $m_h = 125$ GeV and shown the branching ratios as a function of μ_2 for $m_S = 60$ GeV (left plot) and $m_S = 75$ GeV (right plot). In the left panel of Fig. 3, with $m_S = 60$ GeV, the invisible decay $h \to SS$ is open and dominates over all other SM decays except around $\mu_2 \sim m_S$ where the coupling hSS, which is proportional to $(m_S^2 - \mu_2^2)$ (Eq. (28)), gets suppressed and hence the situation becomes similar to the SM. In the case where $h \to SS$ dominates, the partial width of

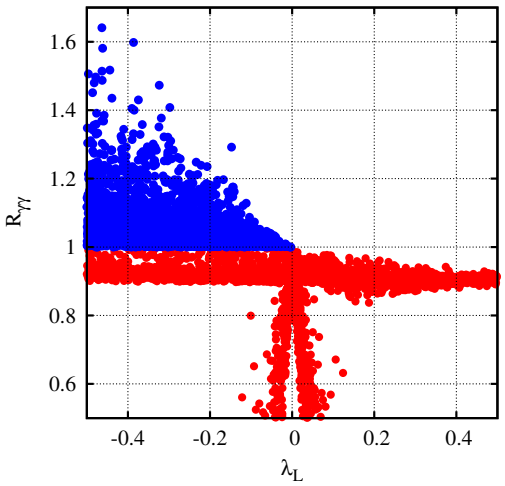

FIG. 2 (color online). $R_{\gamma\gamma}$ as a function of λ_L with the range of parameters as given in Eq. (29).

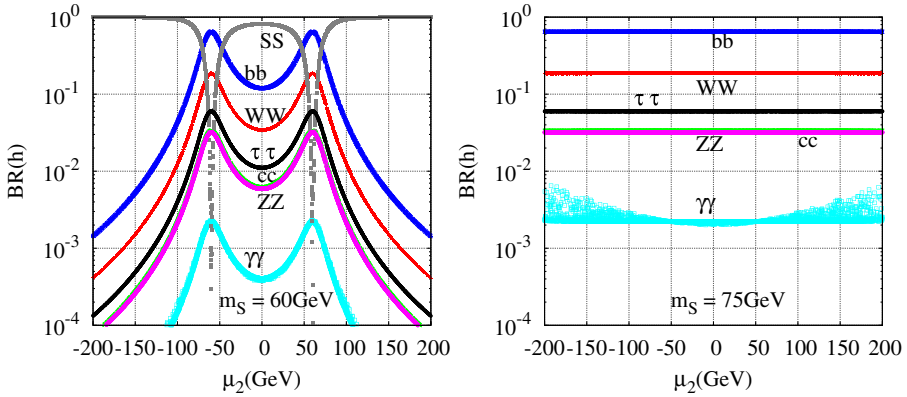

FIG. 3 (color online). Branching ratio of Higgs boson h as a function of μ_2(GeV) in the IHDM with $m_S = 60$ GeV (left panel) and $m_S = 75$ GeV (right panel). We have chosen $m_h = 125$ GeV and have varied other parameters in range $70 < m_{H^\pm}$, $m_A < 1000$, $0 < \lambda_2 < 8\pi$, and $-500 < \mu_2 < 500$.

$h \to SS$ contributes significantly to the total width of the Higgs resulting in a suppression of the Br$(h \to \gamma\gamma)$, which is always smaller than its SM value. For $|\mu_2| \sim m_S$, the Br$(h \to \gamma\gamma)$ can reach the SM value. We can observe from Fig. 3 (left) that the branching fraction of the invisible decay of the SM Higgs $(h \to SS)$ could be very large resulting in a suppression of the other modes, such as $b\bar{b}$, WW, ZZ, and $\tau^+\tau^-$, and hence one can evade the present experimental constraints on the SM Higgs mass based on WW, ZZ, and $\tau^+\tau^-$. The invisible decay of the SM Higgs could evade some of the constraints on the SM Higgs boson that have been extensively studied in many phenomenological studies [30]. We will discuss this in future work [29].

In the right panel of Fig. 3, we take $m_S = 75$ GeV that kinematically closes the decay $h \to SS$. In this case, the total decay width of the Higgs boson is similar in both the SM and IHDM. Therefore, the partial decay width $\Gamma(h \to \gamma\gamma)$ will receive only smooth variation due to the charged Higgs contribution resulting in an enhancement of Br$(h \to \gamma\gamma)$ where up to a factor of 2 over the SM is possible. In our parametrization of the IHDM given in Eq. (7), λ_3 is fixed by the charged Higgs mass and μ_2 through Eq. (6). The sign of λ_3 is then completely fixed by the sign of $m^2_{H^\pm} - \mu_2^2$. Hence, for small $|\mu_2| < m_{H^\pm}$, the sign of λ_3 is positive. In such a case, the charged Higgs contribution to $\Gamma(h \to \gamma\gamma)$ is totally destructive with the SM. While for large $|\mu_2| > m_{H^\pm}$, λ_3 becomes negative and the charged Higgs contribution to $\Gamma(h \to \gamma\gamma)$ becomes constructive with the SM and gets substantial enhancement.

In Fig. 4 (left panel) we have shown $R_{\gamma\gamma}$ as a function of λ_3. The other parameters are taken as specified in Eq. (29). As can be seen from the plot, the IHDM can increase the value of $R_{\gamma\gamma}$ (> 1) only for negative values of λ_3 where the charged Higgs contribution is constructive with the W loops. For positive λ_3, the charged Higgs contribution is destructive with the W loops resulting in a suppression of $h \to \gamma\gamma$ rate. The dependence of $R_{\gamma\gamma}$ on the charged Higgs mass is illustrated in the right panel of Figure. 4. The variation of $R_{\gamma\gamma}$ as a function of $m_{H^\pm}$ scales almost like $1/m^2_{H^\pm}$. Varying $m_{H^\pm}$ between 70 GeV and 190 GeV results in a change of $R_{\gamma\gamma}$ from 1.5 to 1. We stress that even for

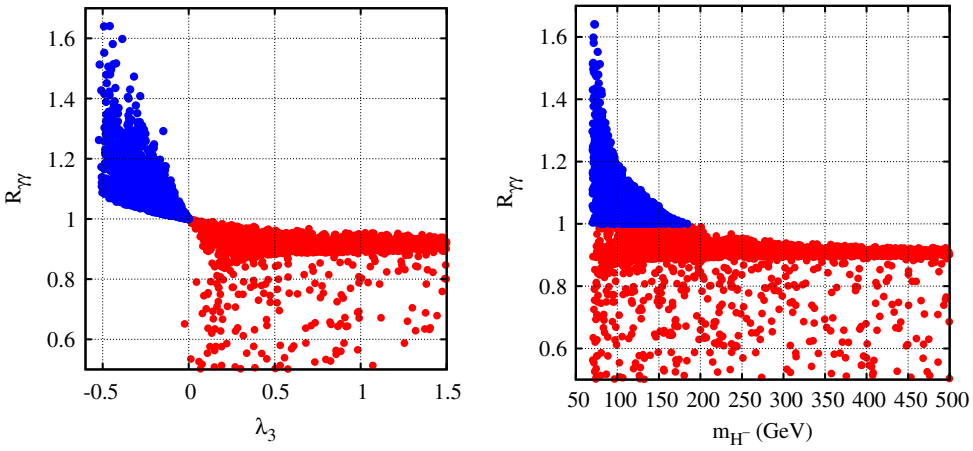

FIG. 4 (color online). Range of values of $R_{\gamma\gamma}$ accessible in the IHD model as a function of λ_3 (left) and $m_{H^\pm}$.

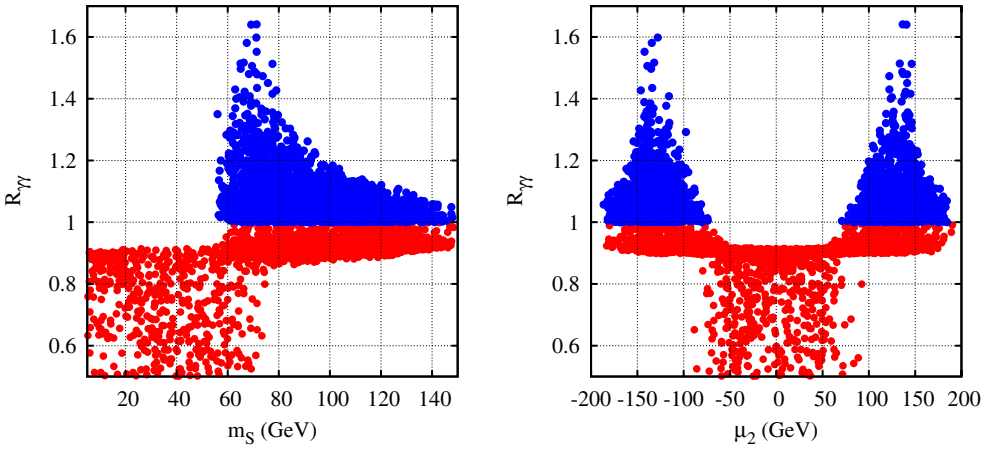

FIG. 5 (color online). Range of values of $R_{\gamma\gamma}$ accessible in the IHD model as a function of m_S (left) and μ_2. The parameter space are the same as in Fig. 1.

light charged Higgs $m_{H^\pm} \in [70, 190]$ GeV, we could have $R_{\gamma\gamma} < 1$. This is due to the possible opening of the invisible decay $h \to SS$ which could significantly reduce the branching fraction of $h \to \gamma\gamma$ or the fact that μ_2 is rather small making λ_3 positive. Note that if we relax the constraint on λ_L discussed above, we can get large λ_3 in the following range: $\lambda_3 \in [-1.5, 2]$. A large and negative $\lambda_3 \sim -1.5$ would give a constructive charged Higgs contribution with the W loops and therefore amplify $R_{\gamma\gamma}$ which can reach 1.6–2.2 for light charged Higgs $\sim 70 - 100$ GeV.

In Fig. 5, we show $R_{\gamma\gamma}$ as a function of m_S and μ_2. From Fig. 5 (left panel) one can observe that an enhancement compared to the SM value in $R_{\gamma\gamma}$ is only possible for $m_S > m_h/2$ while for $m_S < m_h/2$ there is a suppression of $R_{\gamma\gamma}$. Similarly one can observe that $R_{\gamma\gamma}$ can be enhanced with respect to the SM value for the relatively large value of μ_2 while for small $|\mu_2| < 70$ GeV $R_{\gamma\gamma}$ is suppressed.

VI. CONCLUSIONS

To summarize, in this work we have studied $h \to \gamma\gamma$ in the IHDM by imposing vacuum stability, perturbativity, unitarity, and precision electroweak measurements. We have shown that within the allowed range of the IHDM model $h \to \gamma\gamma$ could show substantial deviation from the SM result. Hence the observation of the Higgs boson in $h \to \gamma\gamma$ could help us in constraining the parameter space of the model. We have also shown that observation of $R_{\gamma\gamma} > 1$ or < 1 could rule out a large portion of the allowed parameter space of the IHDM. Taking into account all the constraints defined in Sec. III there is an upper bound on $m_{H^\pm}$ and m_A as evident from Fig. 1 (left panel). This bound essentially comes from unitarity of the model. If the CMS and ATLAS excess in the di-photon channel is confirmed with more data, having $R_{\gamma\gamma} > 1$ would favor the following scenarios:

(i) $\lambda_3 < 0$, i.e., $|\mu_2| > m_{H^\pm}$.
(ii) Charged Higgs boson mass ($m_{H^\pm}$) will be bounded ($\lesssim 200$ GeV).

On the other hand, if with more data we have $R_{\gamma\gamma} < 1$, this scenario would favor either a light DM particle $m_S < m_h/2$ such that $h \to SS$ is open and/or a positive λ_3 i.e., $m_{H^\pm} > |\mu_2|$.

ACKNOWLEDGMENTS

We would like to thank Chuan-Hung Chen and Gilbert Moultaka for useful discussions. A. A would like to thank NSC-Taiwan for partial support during his stay at NCKU where part of this work has been done. The work of R. B was supported by the Spanish Consejo Superior de Investigaciones Cientificas (CSIC). The work of N. G. is supported by grants from Department of Science & Technology (DST), India under Project No. SR/S2/HEP-09/10 and University Grants Commission (UGC), India under Project No. 38-58/2009(SR).

[1] (ATLAS Collaboration), ATLAS Report No. ATLAS-CONF-2011-163.
[2] (CMS Collaboration), CMS Report No. PAS HIG-11-032.
[3] (ATLAS Collaboration), ATLAS Report No. ATLAS-CONF-2011-161.
[4] (CMS Collaboration), CMS Report No. PAS HIG-11-030.

[5] N. G. Deshpande and E. Ma, Phys. Rev. D **18**, 2574 (1978).

[6] M. Gustafsson, E. Lundstrom, L. Bergstrom, and J. Edsjo, Phys. Rev. Lett. **99**, 041301 (2007); T. Hambye and M. H. G. Tytgat, Phys. Lett. B **659**, 651 (2008); E. Lundstrom, M. Gustafsson, and J. Edsjo, Phys. Rev. D **79**, 035013 (2009); P. Agrawal, E. M. Dolle, and C. A. Krenke, Phys. Rev. D **79**, 015015 (2009); E. Nezri, M. H. G. Tytgat and G. Vertongen, J. Cosmol. Astropart. Phys. 04 (2009) 014; S. Andreas, M. H. G. Tytgat and Q. Swillens, J. Cosmol. Astropart. Phys. 04 (2009) 004; C. Arina, F. -S. Ling and M. H. G. Tytgat, J. Cosmol. Astropart. Phys. 10 (2009) 018; L. Lopez Honorez and C. E. Yaguna, J. High Energy Phys. 09 (2010) 046; A. Melfo, M. Nemevsek, F. Nesti, G. Senjanovic, and Y. Zhang, Phys. Rev. D **84**, 034009 (2011).

[7] E. M. Dolle and S. Su, Phys. Rev. D **80**, 055012 (2009).

[8] E. Ma, Phys. Rev. D **73**, 077301 (2006).

[9] R. Barbieri, L. J. Hall, and V. S. Rychkov, Phys. Rev. D **74**, 015007 (2006).

[10] E. Lundstrom, M. Gustafsson, and J. Edsjo, Phys. Rev. D **79**, 035013 (2009).

[11] Q. -H. Cao, E. Ma, and G. Rajasekaran, Phys. Rev. D **76**, 095011 (2007).E. Dolle, X. Miao, S. Su, and B. Thomas, Phys. Rev. D **81**, 035003 (2010).X. Miao, S. Su, and B. Thomas, Phys. Rev. D **82**, 035009 (2010).

[12] B. W. Lee, C. Quigg, and H. B. Thacker, Phys. Rev. D **16**, 1519 (1977); R. Casalbuoni, D. Dominici, R. Gatto, and C. Giunti, Phys. Lett. B **178**, 235 (1986); R. Casalbuoni, D. Dominici, F. Feruglio, and R. Gatto, Nucl. Phys. **B299**, 117 (1988).

[13] S. Kanemura, T. Kubota, and E. Takasugi, Phys. Lett. B **313**, 155 (1993).

[14] A. G. Akeroyd, A. Arhrib, and E. M. Naimi, Phys. Lett. B **490**, 119 (2000); A. Arhrib, J. Horejsi, and M. Kladiva, Eur. Phys. J. C **46**, 81 (2006); B. Gorczyca and M. Krawczyk, arXiv:1112.5086; I. F. Ginzburg and I. P. Ivanov, Phys. Rev. D **72**, 115010 (2005); I. F. Ginzburg and I. P. Ivanov, arXiv:hep-ph/0312374.

[15] M. E. Peskin and T. Takeuchi, Phys. Rev. D **46**, 381 (1992).

[16] K. Nakamura *et al.* (Particle Data Group Collaboration), J. Phys. G **37**, 075021 (2010).

[17] S. Kanemura, Y. Okada, H. Taniguchi, and K. Tsumura, Phys. Lett. B **704**, 303 (2011).

[18] (The ATLAS & CMS Collaborations), ATLAS, Report No. CONF-2011-157/CMS-PAS-HIG-11-023

[19] J. R. Ellis, M. K. Gaillard, and D. V. Nanopoulos, Nucl. Phys. **B106**, 292 (1976); M. A. Shifman, A. I. Vainshtein, M. B. Voloshin, and V. I. Zakharov, Sov. J. Nucl. Phys. **30**, 711 (1979).

[20] A. Djouadi, V. Driesen, W. Hollik, and J. I. Illana, Eur. Phys. J. C **1**, 149 (1998); M. Carena, S. Gori, N. R. Shah, and C. E. M. Wagner, arXiv:1112.3336.

[21] S. Moretti and S. Munir, Eur. Phys. J. C **47**, 791 (2006); U. Ellwanger, Phys. Lett. B **698**, 293 (2011).

[22] P. Posch, Phys. Lett. B **696**, 447 (2011).

[23] A. Arhrib, W. Hollik,S. Penaranda and M. Capdequi Peyranere, Phys. Lett. B **579**, 361 (2004); I. F. Ginzburg, M. Krawczyk, and P. Osland, Nucl. Instrum. Methods Phys. Res., Sect. A **472**, 149 (2001); D. Lopez-Val and J. Sola, Phys. Lett. B **702**, 246 (2011); N. Bernal, D. Lopez-Val, and J. Sola, Phys. Lett. B **677**, 39 (2009).

[24] P. M. Ferreira, R. Santos, M. Sher, and J. P. Silva, Phys. Rev. D **85**, 035020 (2012); P. M. Ferreira, R. Santos, M. Sher, and J. P. Silva, Phys. Rev. D **85**, 077703 (2012).

[25] T. Han, H. E. Logan, B. McElrath, and L. T. Wang, Phys. Lett. B **563**, 191 (2003); **603**, 257 (2004); L. Wang and J. M. Yang, Phys. Rev. D **84**, 075024 (2011).

[26] K. Cheung and T. C. Yuan, Phys. Rev. Lett. **108**, 141602 (2012).

[27] A. Arhrib, R. Benbrik, M. Chabab, G. Moultaka, and L. Rahili, arXiv:1112.5453; P. Fileviez Perez, H. H. Patel, M. J. Ramsey-Musolf, and K. Wang, Phys. Rev. D **79**, 055024 (2009).

[28] A. Djouadi, Phys. Rep. **457**, 1 (2008); A. Djouadi, Phys. Rep. **459**, 1 (2008).

[29] A. Arhrib, R. Benbrik, and N. Gaur, (unpublished).

[30] K. Belotsky, D. Fargion, M. Khlopov, R. Konoplich, and K. Shibaev, Phys. Rev. D **68**, 054027 (2003); Y. Mambrini, Phys. Rev. D **84**, 115017 (2011); M. Raidal and A. Strumia, Phys. Rev. D **84**, 077701 (2011); X. -G. He and J. Tandean, Phys. Rev. D **84**, 075018 (2011); I. Low, P. Schwaller, G. Shaughnessy, and C. E. M. Wagner, Phys. Rev. D **85**, 015009 (2012); C. Englert, J. Jaeckel, E. Re, and M. Spannowsky, Phys. Rev. D **85**, 035008 (2012); Y. Bai, P. Draper, and J. Shelton, arXiv:1112.4496; X. -G. He, B. Ren, and J. Tandean, arXiv:1112.6364; C. Englert, T. Plehn, M. Rauch, D. Zerwas, and P. M. Zerwas, Phys. Lett. B **707**, 512 (2012); A. Djouadi, O. Lebedev, Y. Mambrini, and J. Quevillon, Phys. Lett. B **709**, 65 (2012).